



Imidacloprid elimination by O₃ and O₃/UV: kinetics study, matrix effect, and mechanism insight

Busra Sonmez Baghizade¹ · Ulku Yetis¹ · Filiz B. Dilek¹

Received: 9 January 2020 / Accepted: 18 May 2020 / Published online: 25 May 2020
© Springer-Verlag GmbH Germany, part of Springer Nature 2020

Abstract

The removal of imidacloprid (IMI) from water by ozonation (O₃) and photo-ozonation (O₃/UV) was comparatively studied, paying particular attention to the kinetics, matrix effect, and mechanistic aspects of the processes. The IMI removal by O₃ was considerably enhanced at alkaline pHs, leading to almost complete removal under 20 min with a pseudo-first-order rate constant of 0.2374 min⁻¹ at pH 8.25. Three different matrices, Milli-Q water, full-scale vacuum rotating membrane bioreactor plant effluent (VRMBR WW), and laboratory-scale instantaneous fed-batch reactor bioreactor effluent (Bio WW) spiked with IMI, were tested. The ozonation, coupled with UV, improved IMI removal remarkably regardless of the wastewater matrix, and there occurred a six times decrease in ozonation time requirement for 99% IMI elimination at pH 7.25. The IMI degradation mechanism proved that IMI is an ozone-resistant pollutant and is mainly degraded by OH• via an indirect mechanism. The second-order rate constants for IMI degradation with OH• were calculated as 2.23 × 10¹¹ and 9.08 × 10¹¹ M⁻¹ s⁻¹ for the O₃ alone and O₃/UV processes, respectively. The IMI degradation pathway analysis showed that IMI lost NO₂, HNO₂, and then Cl⁻ from its structure, and the O₃/UV process yielded fewer by-products than O₃.

Keywords Imidacloprid · Ozonation · Photo-ozonation · By-products · Kinetics · Water matrix

Introduction

The removal of thousands of different micropollutants present in wastewater effluents has received increased attention in recent years due to their potential risk to the aquatic environment and human health (Vatankhah et al. 2019, Liu et al. 2020). Since the conventional urban wastewater treatment plants (UWWTPs) are not specifically designed for the removal of these pollutants, their occurrence in the treated effluents and, in turn, in the receiving water bodies has become a widespread problem. Although the regulation of micropollutants in UWWTP effluents is still under discussion at the European level (Rizzo et al. 2018), Switzerland and

Germany (only in two federal states) are implementing advanced treatments for the removal of micropollutants from UWWTP effluents (Cerreta et al. 2019).

The European List of Priority Substances that was defined by the Water Framework Directive (2000/60/EC) was revised in 2013, and 12 new substances and groups of substances were added to the existing list of 33 priority substances (Directive 2013/39/EU). Later, in the year 2018, European Commission published a list of 17 potential water pollutants (known as “2nd Watch List”) that should be carefully monitored by the EU Member States to determine the risk they pose to the aquatic environment (Loos et al. 2018). One of the micropollutants that are included in this watch list is the pesticide imidacloprid (IMI) (1-((6-chloro-3-pyridinyl) methyl)-N-nitro-2-imidazolidinimine (C₉H₁₀ClN₅O₂)) with a widespread occurrence in the EU waters. IMI is one of the major neonicotinoids used for pest control (Dani et al. 2019) and known to pose a particular threat to the environment due to its high solubility (0.58 g L⁻¹), and high persistence in surface waters (Rózsa et al. 2019).

Regarding the removal of IMI from wastewater, there are several literature studies in which various processes, such as adsorption (Mandal and Singh 2017), membrane filtration

Responsible Editor: Vitor Pais Vilar

Electronic supplementary material The online version of this article (<https://doi.org/10.1007/s11356-020-09355-2>) contains supplementary material, which is available to authorized users.

✉ Filiz B. Dilek
fdilek@metu.edu.tr

¹ Department of Environmental Engineering, Middle East Technical University, Dumlupinar Bulvari, 06800 Ankara, Turkey

(Genç et al. 2017), photo-Fenton (Segura et al. 2008), electro-Fenton process (Zhao et al. 2018), photocatalysis (Malato et al. 2002; Kanwal et al. 2018), ozonation (Cernigoj et al. 2007; Bourgin et al. 2011; Chen et al. 2018), electrocatalytic oxidation (Zhang et al. 2020), and cavitation (Raut-Jadhav et al. 2013), were investigated. However, among these processes, ozonation (O_3), as one of the favorable advanced oxidation processes (AOPs), has been considered in very few studies (Reynolds et al. 1989; Oller et al. 2011). Bourgin et al. (2011) studied the degradation of IMI by O_3 and focused only on the sole ozonation, but not catalytic ozonation. The study showed that the IMI degradation is a first-order reaction with respect to ozone. The ozonation by-products were identified, and a degradation pathway was proposed. In another recent study, Chen et al. (2018) also studied the use of sole ozone for IMI degradation and investigated the effect of pH on oxidation kinetics. They indicated that the degradation reaction is pseudo-first-order, and the rate is minimum at pH 6.02. They further reported that the increase in pH from 6.02 to 8.66 causes a 4.1 times increase in the reaction rate. Despite this interest, no one, to the best of our knowledge, investigated the elimination of IMI from waters by the photo-ozonation process (O_3/UV). This work aimed to fill in the existing gap in the literature by providing a comprehensive work on the removal of IMI from waters by O_3 and O_3/UV processes in a comparative manner and by presenting the possible reaction pathway of IMI degradation, as well. We considered the O_3 and O_3/UV processes due to several reasons. First of all, O_3 process is a simple, easy to control, clean, and reliable process. Compared to the other treatment processes, it can be easily incorporated into existing and new WWTPs (Schmitt et al. 2020). Moreover, it provides a chemical-free means of removing micropollutants with high efficiency (Prieto-Rodríguez et al. 2013; Schmitt et al. 2020). Further, the addition of UV irradiation increases the mineralization of recalcitrant organic compounds (Rajah et al. 2019). In this respect, in the present study, laboratory-scale semi-batch tests were conducted to enlighten the effect of different operational parameters such as pH, ozone dose, and initial IMI concentration ($[IMI]_0$) as well as water matrix on the IMI degradation and its kinetics.

Materials and methods

Chemicals

The analytical grade standard of IMI (99.9%) was purchased from Dr. Ehrenstorfer GmbH (Augsburg, Germany). DPD-free chlorine reagent powder pillows (for 25-mL sample) were obtained from Hach. Potassium iodide ($\geq 99\%$ purity), potassium iodate ($\geq 99.7\%$ purity), sodium thiosulfate pentahydrate ($\geq 99.5\%$ purity), starch (iso reagent), tert-butanol ($\geq 99.5\%$

purity), sulfuric acid (95–98% purity), potassium dihydrogen phosphate ($\geq 99.5\%$ purity), dipotassium hydrogen phosphate ($\geq 98\%$ purity), and acetonitrile (gradient grade for liquid chromatography, $\geq 99.9\%$ purity) were purchased from Merck (Darmstadt, Germany). P-Chlorobenzoic acid (pCBA, $\geq 99\%$ purity) was obtained from Sigma-Aldrich (Germany). Milli-Q (type 1) water and pure water (type 3) were prepared using Merck Millipore Milli-Q A10 ultra-pure water purification system (Darmstadt, Germany) and RiOs Essential 16 water purification system (Darmstadt, Germany), respectively.

IMI and IMI concentrations studied

IMI (CAS number of 138261-41-3) is an insecticide that belongs to the neonicotinoid pesticide group (Fig. 1). It is widely used during the production of sugar beet, grape, apple, pear, and tomato. IMI occurs as colorless crystals that are highly soluble in water (0.61 g L^{-1}). It has a low octanol-water coefficient ($\log K_{ow}$) of 0.52 at 21°C and pH 7 (Tomlin 2006). Therefore, IMI can easily reach to water bodies (Jeschke et al. 2010).

During the measurement of IMI at HPLC, LoD was found as $5 \mu\text{g L}^{-1}$, which is much higher than the concentrations observed in the watercourses. So, to be able to measure the concentration of IMI after treatment, it was deemed necessary to work with some higher initial concentrations as such, possibly to give $5 \mu\text{g L}^{-1}$ final concentration with at least 95% removal. In this way, it would be possible to follow the degradation kinetics, as well as the by-product formation. Additionally, possible higher IMI concentrations to be encountered in IMI formulating and manufacturing plants' wastewaters were also taken into consideration while determining the $[IMI]_0$ to study. Thus, the $[IMI]_0$ between 100 and $1000 \mu\text{g L}^{-1}$ was studied.

Wastewater samples

During the experiments, three types of water samples, namely, Milli-Q water and two different secondarily treated urban wastewaters, were used. The former is the ultra-pure water obtained from a Milli-Q water system (Millipore) with a specific resistance of $18.2 \text{ M}\Omega \text{ cm}$. Milli-Q water was used as a control to figure out ozone decomposition factors by eliminating the matrix effect of wastewater and perform a parametric

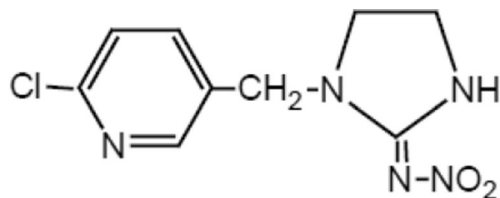


Fig. 1 Molecular structure of IMI

study. This Milli-Q water was spiked with the desired IMI amounts before experimentations.

Two different secondarily treated urban wastewaters were used to understand the matrix effect on the degradation of IMI by O_3 and O_3/UV processes. One of these secondarily treated wastewater effluents was collected from a full-scale Vacuum Rotating Membrane Bioreactor plant (VRMBR), which is in operation at METU Campus, Ankara. The wastewater sample ($COD = 19 \text{ mg L}^{-1}$) was collected in a 30-L bottle and transferred to the laboratory straight away. The other wastewater sample (Bio WW) ($COD = 247 \text{ mg L}^{-1}$) was obtained from a laboratory-scale instantaneous fed-batch reactor (FBR) receiving IMI (as spiked) in its influent. This Bio WW was produced during the study by Kocaman (2019), who operated a lab-scale FBR seeded with activated sludge taken from the wastewater treatment plant of Ankara and acclimated to IMI. After acclimation, various concentrations of IMI were spiked to the reactor and treated biologically. Both the Bio WW and VRMBR samples collected in polyethylene bottles were filtered through a $0.45\text{-}\mu\text{m}$ Millipore membrane filters via a vacuum filtration unit within 24 h after sampling. After filtration, treated wastewater was poured into 2.5-L amber glass bottles that were previously washed with Alconox and rinsed thoroughly with tap water, pure water, and Milli-Q water, respectively, and then stored in a refrigerator at $+4 \text{ }^\circ\text{C}$ in the dark. The filtration was applied to remove impurities, which may cause clogging of the HPLC column and avert inaccurate measurements during the analysis of samples. The filtered VRMBR sample was spiked with IMI at desired concentrations before experimentations.

Experimental setup

In the experiments, the laboratory-scale O_3 and O_3/UV systems that are composed of an ozone generator, O_3 , or O_3/UV cylindrical borosilicate glass reactors (volume 1 L) and gas washing bottle were used. Ozone was produced from the air using an ozone generator (WEDECO OCS-Modular 4 HC - AirSep AS 12) supplying a maximum ozone production rate of 4 g h^{-1} at 0.5 bar. Concentration and flowrate of the output ozone gas can be adjusted between 0 to 200 mg L^{-1} and 10 to 140 L h^{-1} , respectively. The ozone was continuously bubbled at a set gas flow rate through a fritted spherical glass diffuser from the bottom of the reactor. The gas washing bottle that contains 500 mL of 2% KI solution $2 \text{ N H}_2\text{SO}_4$ was placed to determine the amount of escaped ozone from the reactor. During O_3/UV treatment, the reactor was stirred by a magnetic stirrer and the temperature was maintained at $24 \pm 0.1 \text{ }^\circ\text{C}$ by circulating water through the cooling jacket of the reactor. In the case of the O_3/UV application, a 10-W UV lamp with a monochromatic emission at a wavelength of 254 nm was placed into a quartz tube that was immersed vertically at the

center of the reactor. The average UV light intensity was measured as $12.2 \times 10^{-3} \text{ }\mu\text{Einstein cm}^{-2} \text{ s}^{-1}$.

Experiments

Experimental conditions implemented during the O_3 and O_3/UV experiments are presented in Table 1. As seen, throughout the experiments, the temperature and the ozone flowrate were kept at $24 \pm 1 \text{ }^\circ\text{C}$ and 30 L h^{-1} , respectively, while the $[\text{IMI}]_0$, ozone dose, and pH were varied. The aimed pHs were adjusted with the use of a phosphate buffer solution. The pH range was selected as 6.25 to 8.25, considering the pH range applied by Chen et al. (2018). The deviation of pH between the aimed and the measured values was less than ± 0.1 unit. The effects of operational parameters (pH, $[\text{IMI}]_0$, and ozone dose) on the IMI removal by O_3 were searched through the experiment sets of 1 to 8. The effect of the water matrix on the degradation of IMI by O_3 (experiment set no: 8, 9, and 10) and O_3/UV (experiment set no: 11, 12, and 13) was investigated using three different water samples as described in the “Wastewater samples” section.

To understand if the mechanism of IMI degradation is direct or indirect, tert-butanol (TBA) which is a well-known $\text{OH}\cdot$ scavenger (Hoigne and Bader 1983) was spiked into the Milli-Q water at concentrations of 100 and 200 mM to inhibit $\text{OH}\cdot$ reactions during O_3 and O_3/UV experiments (experiment set no: 14 and 15), respectively. Since UV irradiation enhances $\text{OH}\cdot$ production, to inhibit $\text{OH}\cdot$ adequately, more TBA was added during O_3/UV experiments. Further, in order to evaluate indirect reaction kinetics of IMI with $\text{OH}\cdot$, a reference compound of p-chlorobenzoic acid (pCBA) at a concentration of $5 \text{ }\mu\text{M}$ was spiked into the Milli-Q water during the O_3 and O_3/UV experiments (experiment set no: 16 and 17, respectively).

Throughout the experiments, ozonated samples (10 mL) were collected at different treatment times from 0 to 180 min, with appropriate intervals allowing to observe not only IMI degradation but also production and removal of degradation by-products, if any. Each sample was urgently quenched with N_2 gas for 5 min to stop the further reaction between IMI and ozone before the HPLC analysis. Also, an additional sample of 5 mL was withdrawn from the reactor for the measurement of dissolved ozone and pH.

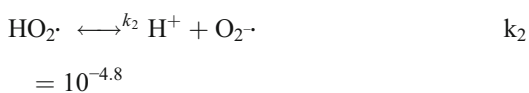
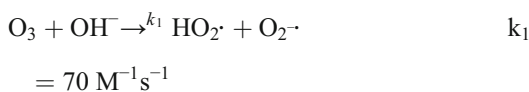
Ozonation reactions and kinetics

The O_3 decomposition occurs with chain reactions, including initiation, propagation, and termination steps (Staelin and Hoigne 1982). Ozone decomposition starts with the attack of OH^- to ozone and this rate-determining step leads to the formation of one superoxide radical ion ($\text{O}_2^{\cdot-}$) and one hydroperoxyl radical $\text{HO}_2\cdot$ (Eq. 1). The second equation represents the regeneration of $\text{O}_2^{\cdot-}$ since $\text{HO}_2\cdot$ is in acid-base

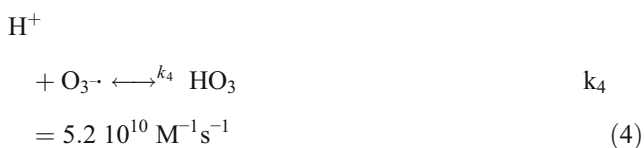
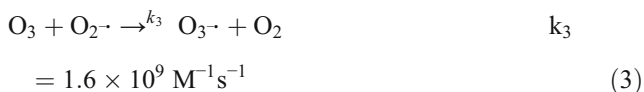
Table 1 Experimental conditions

Set no.	Water matrix	pH	Temperature (°C)	Initial IMI ($\mu\text{g L}^{-1}$)	O ₃ dose (mg h^{-1})	O ₃ flowrate (L h^{-1})	UV light (10 W)	TBA (mM)	pCBA (5 μM)
Effect of operational parameters (O ₃)									
1	Milli-Q	6.20 ± 0.1	24 ± 1	500	1200	30	No	No	No
2	Milli-Q	7.25 ± 0.1	24 ± 1	500	1200	30	No	No	No
3	Milli-Q	8.25 ± 0.1	24 ± 1	500	1200	30	No	No	No
4	Milli-Q	7.25 ± 0.1	24 ± 1	500	600	30	No	No	No
5	Milli-Q	7.25 ± 0.1	24 ± 1	500	1200	30	No	No	No
6	Milli-Q	7.25 ± 0.1	24 ± 1	500	1800	30	No	No	No
7	Milli-Q	7.25 ± 0.1	24 ± 1	100	1200	30	No	No	No
8	Milli-Q	7.25 ± 0.1	24 ± 1	1000	1200	30	No	No	No
Effect of water matrix (O ₃)									
8	Milli-Q	7.25 ± 0.1	24 ± 1	1000	1200	30	No	No	No
9	VRMBR WW	7.25 ± 0.1	24 ± 1	1000	1200	30	No	No	No
10	Bio WW	7.25 ± 0.1	24 ± 1	332	1200	30	No	No	No
Effect of water matrix (O ₃ /UV)									
11	Milli-Q	7.25 ± 0.1	24 ± 1	1000	1200	30	Yes	No	No
12	VRMBR WW	7.25 ± 0.1	24 ± 1	1000	1200	30	Yes	No	No
13	Bio WW	7.25 ± 0.1	24 ± 1	332	1200	30	Yes	No	No
Mechanism of degradation (O ₃)									
14	Milli-Q	7.25 ± 0.1	24 ± 1	1000	1200	30	No	100	No
Mechanism of degradation (O ₃ /UV)									
15	Milli-Q	7.25 ± 0.1	24 ± 1	1000	1200	30	Yes	200	No
Second-order kinetics study									
16	Milli-Q	7.25 ± 0.1	24 ± 1	1000	1200	30	No	No	Yes
17	Milli-Q	7.25 ± 0.1	24 ± 1	1000	1200	30	Yes	No	Yes

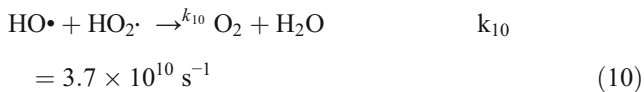
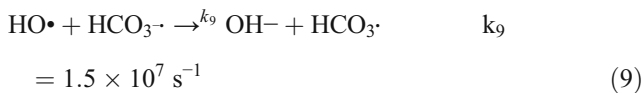
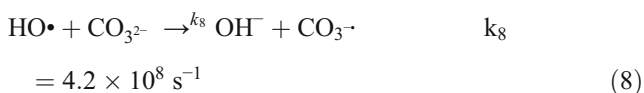
equilibrium with O₂^{-•} (Staehelin and Hoigne 1982).



The propagation step includes ozonide anion (O₃^{-•}) production by the attack of ozone to O₂^{-•}. Further reactions constitute OH• (Eqs. 3–7) (Staehelin and Hoigne 1982).



Several organic and inorganic compounds react with OH• to form secondary radicals which do not further form superoxide radicals such as HO₂[•] and O₂^{-•} (Eq. 8 and Eq. 9) (Staehelin and Hoigne 1982). These compounds are generally named as scavengers or inhibitors since they inhibit ozone decay and, in turn, radical production. Another possibility for scavenging radicals can be the reaction of two radicals (Eq. 10).



The ozonation reaction kinetics is second-order since both O₃ and OH• oxidize the IMI. The overall reaction kinetics can be described as follows:

$$-\frac{d[\text{IMI}]}{dt} = k_{\text{OH}\cdot\text{-IMI}}[\text{IMI}][\text{OH}\cdot] + k_{\text{O}_3\text{-IMI}}[\text{IMI}][\text{O}_3] \quad (11)$$

where [IMI] is the concentration of IMI, [OH•] is the concentration of OH•, [O₃] is the concentration of O₃, k_{OH•-IMI} is the second-order rate constant of OH• with IMI, and k_{O₃-IMI} is the second-order rate constant of O₃ with IMI.

During ozonation experiments, ozone was excessively supplied into the system with respect to IMI concentration. So, the reaction rate of ozonation mainly depended on the concentration of IMI. The ozonation reactions followed pseudo-first-order kinetics, which was also supported by the linear plot with a high R² value obtained by plotting the -ln(C/C₀) vs the time graph. The direct ozonation of IMI was exhibited pseudo-first-order reaction, as follows:

$$-\frac{d[\text{IMI}]}{dt} = k_{\text{app}} [\text{IMI}] \quad (12)$$

where [IMI] is the concentration of IMI and k_{app} is the apparent pseudo-first-order rate constant (k_{app} = k_{OH•-IMI} + k_{O₃-IMI}).

Analytical methods

The analysis of IMI and its degradation by-products was performed via an Agilent 1200 high-performance liquid chromatography (HPLC) system equipped with a UV detector and a ZORBAX Rapid Resolution Eclipse Plus C18 column (4.6 × 100 mm, 3.5 μm). The IMI detection was performed at 270 nm. The mobile phase flow rate, column oven temperature, and injection volume were 0.5 mL min⁻¹, 30 °C, and 20 μL, respectively. The elution was performed under the following gradient conditions, where A is the acetonitrile and B is the Milli-Q water: t = 0 min, A–B (20:80, v/v); t = 0.1 min, A–B (20:80, v/v); t = 4.0 min, A–B (50:50, v/v); t = 7.0 min, A–B (20:80, v/v); t = 10 min, A–B (20:80, v/v). The limit of detection (LoD) and limit of quantification (LoQ) were calculated as 5 and 16.9 μg L⁻¹, respectively. Data

acquisition and processing were performed with the Chemstation software.

The possible degradation by-products were analyzed by an AGILENT 6460 LC/MS/MS Triple Quadrupole System (ESI+Agilent Jet Stream) operated in the multiple reaction monitoring (MRM) mode with dynamic time segment acquisition windows coupled with AGILENT 1200 Series HPLC equipped with Poroshell 120 SB-C18 (3 × 100 mm, 1.2 μm) column. The mobile phase flow rate, column oven temperature, and injection volume were 0.3 mL min⁻¹, 65 °C, and 1 μL, respectively. The mobile phase was composed of 5% water and 95% acetonitrile. The mass spectrometer was operated in positive ion ESI mode, using the capillary voltage 400 V, sheat gas flow 9 mL min⁻¹, nozzle voltage 1500 V, sheat gas temperature 300 °C, and nitrogen as desolvation/nebulization gas generated by Nitrogen generator UHPLCMS 30. Data acquisition and processing were performed with the AGILENT G3793AA, Mass Hunter Optimizer software.

Detection of pCBA was performed by Agilent 1200 HPLC with a ZORBAX Rapid Resolution Eclipse Plus C18 column (4.6 × 100 mm, 3.5 μm) using 60% methanol and 40% Milli-Q water (adjusted to pH 2 using 10 mM H₃PO₄) at 1 mL min⁻¹ flowrate and UV detection at 240 nm. The column oven temperature and injection volume were 30 °C and 100 μL, respectively. The LoD was 5 μg L⁻¹.

The dissolved ozone concentration in the reactor was measured spectrophotometrically via the Hach method 10069. The ozone escaped from the reactor was captured in a gas washing bottle and measured using the iodine method (Rackness et al. 1996). The pH was measured with a Hach HQ40D portable multimeter (Hach, USA). The average UV light intensity was measured using the iodide–iodate (KI/KIO₃) actinometer method (Bolton et al. 2011).

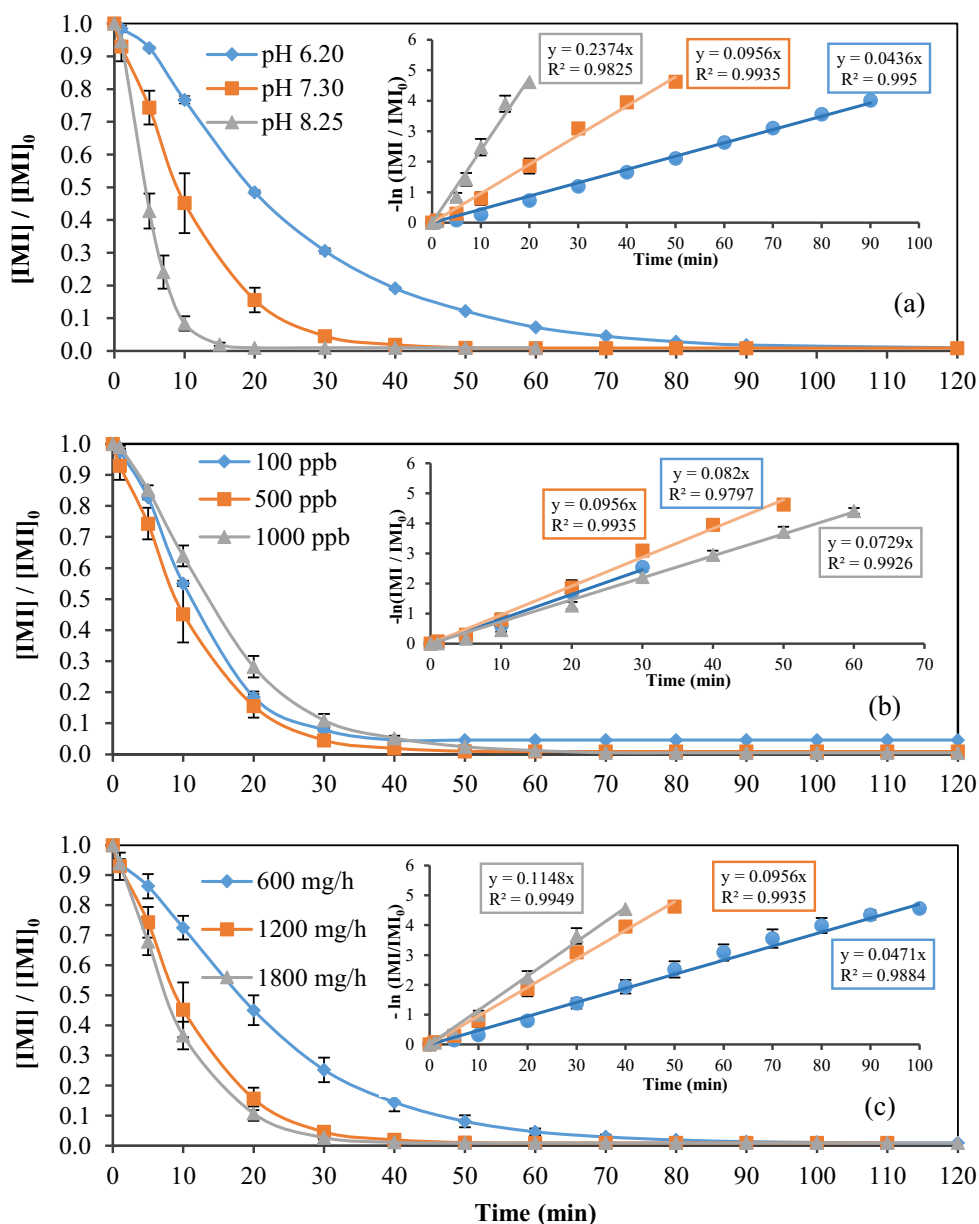
Results and discussion

Effect of pH, ozone dose, and [IMI]₀ on IMI removal by ozonation

Figure 2 a, b, c, and d show the effects of pH, [IMI]₀, ozone dose, and applied ozone amount on the IMI removal, respectively. In general, the degradation immediately started as the ozone was introduced into the system. There occurred two phases of IMI disappearance: a rapid decrease in IMI, followed by a gradual decline.

As seen from Fig. 2a, the solution pH was an important operational parameter, and the highest removal efficiency was achieved at pH 8.25, whereas the lowest was at pH 6.20. During the first 30 min of the ozonation, IMI removal efficiencies were 69%, 95%, and 99% at pH 6.20, 7.25, and 8.25, respectively. Furthermore, 60 min and 20 min were enough to

Fig. 2 Effect of **a** pH (Milli-Q water, $[IMI]_0 = 500 \mu\text{g L}^{-1}$, O_3 dose = 1200 mg h^{-1} , O_3 flowrate = 30 L h^{-1} , $T = 24 \pm 1 \text{ }^\circ\text{C}$); **b** $[IMI]_0$ (Milli-Q water, O_3 dose = 1200 mg h^{-1} , O_3 flowrate = 30 L h^{-1} , pH = 7.25 ± 0.1 , $T = 24 \pm 1 \text{ }^\circ\text{C}$); **c** O_3 dose (Milli-Q water, $[IMI]_0 = 500 \mu\text{g L}^{-1}$, O_3 flowrate = 30 L h^{-1} , pH = 7.25 ± 0.1 , $T = 24 \pm 1 \text{ }^\circ\text{C}$)



reach 99% (<LoD) disappearance of IMI at pHs 7.25 and 8.25, respectively, while at least 120-min ozonation was required for the same degree of IMI degradation at pH 6.20.

The kinetic analysis showed that the IMI removal by O_3 follows pseudo-first-order kinetics. The apparent rate constants calculated (Fig. 2a) proved that the degradation of IMI was much slower at pH 6.20 compared to other pHs. Indeed, it was found that the increase of the solution pH from 6.20 to 7.25 caused 2.2 times to increase in the IMI disappearance rate. When pH was 8.25, it was also obtained that the kinetic rate constant was more than doubled at even one-unit increase in the pH scale. The IMI disappearance rate at basic pH is almost 5.4 times faster than at acidic pH. This observation could be attributed to the role of OH^\bullet during the initiation

reaction (Eq. 1) and chain reaction, which produces radicals, as stated by Staehelin and Hoigne (1982). As the concentration of OH^\bullet gets higher in alkaline solution, more radicals that also have a high oxidizing capacity are produced. Therefore, as the pH gets higher, IMI removal efficiency increases due to degradation by both ozone and radicals. On the other hand, at acidic pHs, the rate of ozone decomposition and radical formation are very slow, so the degradation of IMI was mainly by ozone itself. Similar results have also been reported by Chen et al. (2018). They reported that the lowest IMI ozonation rate was observed at pH 6.02, and the increase in pH from 6.02 to 8.66 increases the rate almost 4.1 times. Similar results were reported by Cernigoj et al. (2007) for the Thiacloprid removal by ozonation. Thiacloprid is one of the pesticides that belongs

to a neonicotinoid chemical group like IMI. In their study, the disappearance rate of Thiocloprid increased almost 8 times when pH was increased from 5.50 to 11.0. Another ozonation study conducted to degrade two pesticides (Bromoxynil and Trifluralin) by Chelme-Ayala et al. (2010) also revealed similar results. For example, at pH 2, 98% of Bromoxynil and 50% of Trifluralin were degraded within 2 and 5 min of ozonation, respectively, also indicating that Trifluralin is highly robust to ozone attack since direct reaction dominates at acidic pH. Trifluralin has high electronegativity since it contains 3 fluorine which eventually results in resistance toward ozone during the ozonation process. Moreover, IMI showed similarity to Trifluralin in terms of electronegativity since IMI has a chloro-pyridine ring, which is known as a highly electronegative moiety. Therefore, it can be said that at acidic pHs, the removal of ozone-resistant chemicals is less efficient since the degradation mainly depends on the direct reaction mechanism. On the other hand, at pH 7, although the degradation rate of both Bromoxynil and Trifluralin increased, degradation rate differences were more noticeable for Trifluralin (Chelme-Ayala et al. 2010). Indeed, the disappearance of IMI also showed significant improvement even at a one-unit change in the pH scale. As the ozone-resistant chemicals are generally found to be highly removable at alkaline conditions, it can be safe to state that IMI is highly removed at alkaline conditions.

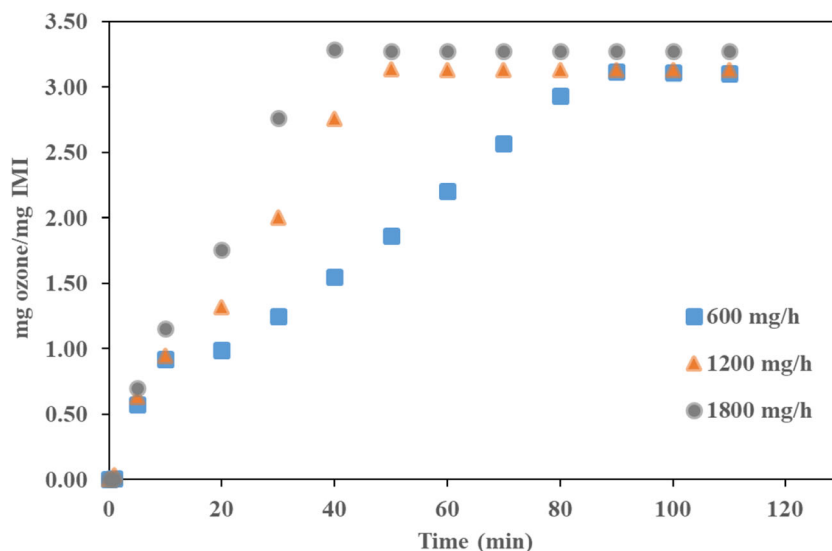
Regarding the effect of the $[IMI]_0$ on the reaction kinetics, nearly 95%, 98%, and 95% IMI disappearance were observed for 100, 500, and 1000 $\mu\text{g L}^{-1}$ $[IMI]_0$, respectively, after 40-min ozonation (Fig. 2b). The apparent rate constant at pH 7.25 was calculated as 0.0820, 0.0956, and 0.0729 min^{-1} for the $[IMI]_0$ of 100, 500, and 1000 $\mu\text{g L}^{-1}$, respectively, the average being 0.0835 min^{-1} . This rate constant is similar to the rate constant reported by Chavez et al. (2019) for the ozonation of 12 micropollutants. Slightly different rate constants observed with different $[IMI]_0$ were thought to originate from the ozonation of by-products. It should be noted that as the $[IMI]_0$ increases, the concentration of degradation by-products also increases. It is well-known that besides micropollutants, degradation by-products may consume available ozone, as well. So, available ozone was used for both IMI and its by-products degradation. Therefore, during ozonation experiments of 1000 $\mu\text{g L}^{-1}$ IMI, there was a pronounced decrease in the rate constant with respect to other concentrations.

Besides pH and $[IMI]_0$, the ozone dose strongly affected the IMI removal rate. As seen from Fig. 2c, the IMI disappearance rate increased with the increase in ozone dose. The increase in the ozone dose from 600 to 1200 mg h^{-1} provided a pronounced increase in the reaction rate constant. As the ozone dose was doubled (from 600 to 1200 mg h^{-1}), the reaction rate also doubled from 0.0471 to 0.0956 min^{-1} . It confirms previous results reported by Bourgin et al. (2011), where an increase in rate constants with increasing ozone dose was

found. The rate constants were calculated as 0.036, 0.071, and 0.129 min^{-1} when the applied ozone concentrations were 25, 50, and 100 g m^{-3} , respectively. On the other hand, the increase of ozone dose from 1200 to 1800 mg h^{-1} did not significantly affect the reaction rate since it increased from 0.0956 to 0.1148 min^{-1} (Fig. 2c). It is worth to mention here that these results could be an indication of a rate-limiting step of the initiation reaction (Eq. 1). Since IMI disappearance mainly depends on the $\text{OH}\cdot$ formation, rate-limiting step may have caused to less $\text{OH}\cdot$ production and hence less increase in rate kinetics when ozone dose increased from 1200 to 1800 mg h^{-1} as compared to ozone dose increased from 600 to 1200 mg h^{-1} . So, the obtained kinetic rates showed that the increase in the ozone dose caused the overall enhancement of the reaction rate. Although the reaction rate was proportionally increased up to 1200 mg h^{-1} ozone dose, after that point, the same correlation was not followed.

Figure 3 shows the variation of specific O_3 consumption by IMI as a function of the cumulative ozone amount applied. The required ozone amount to remove almost all IMI from the solution was observed to be about 3.25 $\text{mg ozone per mg IMI removed}$. However, specific O_3 consumption was very rapid at 1800 mg h^{-1} O_3 application rate. As shown, the IMI removal was almost complete at the dose of 1800 mg h^{-1} in 40 min, whereas it was nearly 110 min at the dose of 600 mg h^{-1} . As previously mentioned, the same amount of ozone was applied to attain the same degree of IMI removal at both 600 and 1200 mg h^{-1} ozone dose. Nevertheless, 600 mg h^{-1} ozone dose required two times longer degradation time than 1200 mg h^{-1} ozone dose. Indeed, this could be considered as expected since the increase in ozone dose provides faster removal of IMI as the applied ozone amount was higher. However, when 1200 and 1800 mg h^{-1} ozone doses were compared, 1200 mg h^{-1} ozone dose required only 10 more min to remove almost all of IMI. Although removing 99% of IMI by 1200 mg h^{-1} ozone dose takes a little bit more time, the applied ozone amount was lower than the one for 1800 mg h^{-1} ozone dose. Hence, this proves that after some point, increasing the ozone dose did not affect the removal efficiency dramatically. The reason for this observation may lie behind the values of reaction rate constants during the production of $\text{OH}\cdot$. The rate constant for the initiation reaction between O_3 and OH^- (Eq. 1) was determined as 70 $\text{M}^{-1} \text{s}^{-1}$ by Staehelin and Hoigne (1982). On the contrary, following radical propagation reactions rate constants are at least five orders of magnitude larger than for Eq. 1. Although ozone dose was increased from 1200 to 1800 mg h^{-1} , the $\text{OH}\cdot$ formation was not increased proportionally since the

Fig. 3 Specific ozone consumption by IMI at different ozone application rates (Milli-Q Water, $[IMI]_0 = 500 \mu\text{g L}^{-1}$, O_3 flowrate = 30 L h^{-1} , $\text{pH} = 7.25 \pm 0.1$, $T = 24 \pm 1 \text{ }^\circ\text{C}$)



initiation reaction (Eq. 1) is the rate-limiting step. Therefore, the removal of IMI did not enhance proportionally as the ozone dose increased from 1200 to 1800 mg h^{-1} . Therefore, 1200 mg h^{-1} ozone dose seems to be more appropriate to apply in practice.

O_3 versus O_3/UV

Since the single ozonation process required long treatment time for IMI degradation, it was considered necessary to apply UV irradiation to enhance IMI removal. The improvement of treatment efficiencies by coupling ozone with UV irradiation was proved for micropollutant removal (Cernigoj et al. 2007) and wastewater treatment studies, as well (Lucas et al. 2010). In this part, the results obtained from the O_3/UV experiments are provided and discussed in the light of similar literature studies to have a deeper understanding of the photo-ozonation of IMI. With this target, the effect of the wastewater matrix on IMI degradation during the O_3/UV process and reaction kinetics were given comparatively with the ozonation process. Possible by-products' production pathway was also demonstrated and discussed explicitly in the following sections.

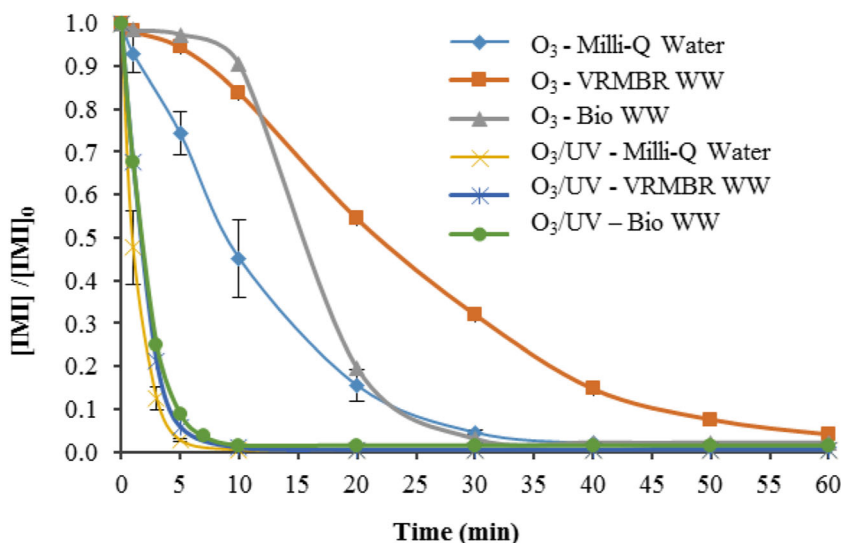
Effect of water matrix

The effectiveness of ozone oxidation depends on both micropollutant reaction with ozone and ozone consumption by water matrix (Gardoni et al. 2012). Indeed, the water matrix strongly affects the removal efficiency of micropollutants, especially O_3 resistant ones (Acero and Von Gunten 2001). To the best of our knowledge, no literature study investigated IMI removal in different water matrices. Yet, the water matrix effect on micropollutant degradation has been widely investigated for pharmaceuticals and other pesticides. Benitez et al.

(2009) investigated several pharmaceuticals (metoprolol, naproxen, amoxicillin, and phenacetin) removal in different water matrices such as groundwater, reservoir water, and 3 different wastewater effluents obtained by municipal treatment plants of Alcalá, Badajoz, and Mostoles in Spain. Almost complete disappearance of phenacetin was observed at groundwater and reservoir water at 3 mg L^{-1} ozone dose. On the other hand, at most 50% phenacetin removal was observed in all wastewaters at the same ozone dose. Moreover, they also noted that as the COD and TOC of wastewaters increases, the removal efficiency decreases. In accordance, Antoniou et al. (2013) investigated the removal of 42 pharmaceuticals in 6 different wastewater matrices. All the micropollutants in the wastewater, which has high COD (90 mg L^{-1}) and alkalinity values ($250 \text{ mg HCO}_3^- \text{ L}^{-1}$) were removed up to 50%. Besides, higher removal rates (50–100%) were observed in the wastewaters that have relatively lower COD values, such as 30 mg L^{-1} .

Figure 4 shows the time-dependent IMI degradation by the O_3/UV process, compared with O_3 , in different water matrices, namely, Milli-Q water, VRMBR WW, and Bio WW. When the results obtained for different water matrices with the application of O_3 only are examined it can be seen that the disappearance of IMI in Milli-Q water started even at the very beginning of ozonation. In addition, among these water matrices, the fastest IMI disappearance was observed in Milli-Q water, as expected. On the other hand, the remarkable difference between Milli-Q water and real wastewaters was a delay in the degradation of IMI in real wastewaters. Wastewaters contain organic constituents such as proteins, carbohydrates, and humic acids and inorganic matters like carbonate and bicarbonate ions which are known as major oxidant consumers since they consume dissolved O_3 (Phattarapattamawong et al. 2017; Gomes et al. 2017). Moreover, the presence of these compounds causes radicals

Fig. 4 Time course variation of IMI concentration at different water matrices. ($[IMI]_0 = 1000 \mu\text{g L}^{-1}$ for Milli-Q water and VRMBR WW, $[IMI]_0 = 332 \mu\text{g L}^{-1}$ for Bio WW, UV lamp = 10 W (where applicable), O_3 dose = 1200 mg h^{-1} , O_3 flowrate = 30 L h^{-1} , $\text{pH} = 7.25 \pm 0.1$, $T = 24 \pm 1 \text{ }^\circ\text{C}$)



scavenging since they also deplete the available $\text{OH}\cdot$ (Ribeiro et al. 2015). Chloride which might exist in the wastewater samples, is a possible $\text{OH}\cdot$ scavenger (Oktem et al. 2019) too. Fijolek and Nawrocki (2018) indicated that chloride even at the concentration of 3.22 mM, which is well above the typical domestic wastewater chloride content (11.3 mM) (Henze 1992) totally blocks ozone decomposition. However, the presence of phosphates in the wastewater samples may overcome the inhibiting effect of chlorides, as reported by Fijolek and Nawrocki (2018). Therefore, this might be the reason for not observing the complete blockage of ozone decomposition due to chloride in our case. As contrary to Fijolek and Nawrocki (2018), Fernandes et al. (2020) reported enhanced paraben removal in the presence of Cl^- , SO_4^{2-} , and HCO_3^- and indicated controversial results reported in the literature. They concluded that the reaction between hydroxyl radicals with these ions produce other radicals that still have high oxidizing potential and may have a higher affinity toward some molecules.

As seen in Fig. 4, at the very beginning of ozonation, the wastewaters consume available ozone and radicals, which eventually caused a delay in the IMI disappearance as compared to Milli-Q water. During the first 10 min of ozonation, nearly 36%, 18%, and 10% of IMI were degraded for Milli-Q water, VRMBR WW, and Bio WW, respectively. The higher IMI removal, though slightly, from VRMBR WW than Bio WW could be attributed to the lower COD of VRMBR WW (19 mg L^{-1}).

Another difference between these two real wastewater samples is that the IMI concentration of the Bio WW ($332 \mu\text{g L}^{-1}$) is lower than that of VRMBR WW ($1000 \mu\text{g L}^{-1}$). As discussed above, an increase in the $[IMI]_0$ increases the rate of IMI oxidation. Since Bio WW has the least IMI concentration, 97.8% IMI disappearance was observed within almost 30 min. On the other hand, at least 70 and 90 min were

required for 99.5% disappearance in Milli-Q water and VRMBR WW, respectively. Although these durations are approximate, the removal difference between Milli-Q water and VRMBR WW matrices were apparent from the very beginning to 50th min ozonation. As proved in our study (“Effect of pH, ozone dose, and $[IMI]_0$ on IMI removal by ozonation” section), the impact of $\text{OH}\cdot$ on IMI disappearance is discernable. Indeed, the reason for disappearance differences might be due to the presence of organics and inorganics in the wastewaters that act as a radical scavenger (Nakada et al. 2007).

The abovementioned negative effect of the real wastewater matrix was removed when UV is coupled with O_3 (Fig. 4). As seen from this figure, the removal of IMI from all studied water matrices was greatly improved when UV was coupled with ozonation. Indeed, the improvement was clearly seen from the very beginning of the O_3/UV process. For instance, within the first 3 min of treatment, 87.4%, 78.9%, and 75.0% of IMI were degraded in Milli-Q water, VRMBR WW, and Bio WW, respectively. After a 10-min process, the removal increased to 99.5% (<LoD), 99.0%, and 96.4%, respectively. By that time, the fastest IMI disappearance was observed for Milli-Q water, as expected, and VRMBR WW showed slightly better removal than Bio WW.

At the end of 20 min of O_3/UV application, IMI disappearance (<LoD) was observed for all wastewater matrices. Indeed, it was clearly seen that the wastewater matrices do not significantly affect IMI removal since the removal rates were very near throughout the process. Hence, it can be said that IMI removal was enhanced by the addition of UV irradiation regardless of the water matrix. Our findings are following the results obtained by Yao et al. (2018). They showed that micropollutants removal from different matrices (surface water, groundwater, and secondary effluent wastewater) were improved regardless of the water matrices by O_3/UV application compared to single ozonation. The reason behind this

incident could be that the ozone decomposition rate, in turn, the production rate of OH• and other radicals were quite enhanced under UV irradiation, although wastewaters have OH• scavenging capacity (Stahelin and Hoigne 1982).

Reaction kinetics

The kinetics of IMI degradation by the O₃/UV process in different water matrices was studied and compared with O₃. It was seen that the degradation kinetics of IMI followed pseudo-first-order kinetics (Fig. 5).

In the O₃/UV process, the apparent rate constants for water matrices Milli-Q, VRMBR WW, and Bio WW were calculated as 0.5768, 0.4833, and 0.4441 min⁻¹, respectively. During the O₃/UV process, the rate constant for Milli-Q water was slightly higher than those for the wastewater samples, as expected. On the other hand, as compared to O₃ alone, O₃/UV process apparently increased the rate constants regardless of water matrices. Indeed, the reaction rate constants of the O₃/UV process were 8.0, 8.7, and 4.6 times higher than those obtained during ozonation in Milli-Q, VRMBR WW, and Bio WW, respectively. The reason behind this remarkable improvement at rate constants is most likely due to the OH• and other radicals' production, which was quite enhanced under UV irradiation (Stahelin and Hoigne 1982). These findings confirmed that IMI degradation kinetics strongly depend on OH• in the solution. Furthermore, the idea that the O₃/UV process highly enhanced the degradation of ozone-resistant micropollutants (Chen et al. 2016) was also proved in our study.

Moreover, the indirect reaction rate constant of photo-ozonation was investigated by a reference compound, namely pCBA and competition kinetics method was used to determine the second-order rate constants for the reactions of IMI with OH•, since the OH• cannot be measured directly during

ozonation and O₃/UV processes. pCBA which is a well-known reference compound is widely applied to measure OH• indirectly. Also, the measurement of the probe compound, pCBA, is rather easy since it can be easily detected by HPLC. The pCBA reacts only OH• ($k_{\text{OH}\cdot\text{-pCBA}} = 5 \times 10^9 \text{ M}^{-1} \text{ s}^{-1}$) and does not considerably react with other radicals or O₃ ($k_{\text{O}_3\text{-pCBA}} = 0.15 \text{ M}^{-1} \text{ s}^{-1}$) (Elovitz and von Gunten 1999). For that purpose, 5 μM pCBA was introduced into Milli-Q water at pH 7.25 ± 0.1 in O₃ and O₃/UV processes.

The kinetics of IMI degradation by OH• can be described as follows:

$$-\frac{d[IMI]}{dt} = k_{\text{OH}\cdot\text{-IMI}}[IMI][\text{OH}\cdot] \quad (13)$$

where $k_{\text{OH}\cdot\text{-IMI}}$ is the second-order rate constant of OH• with IMI, [IMI] is the concentration of IMI, and [OH•] is the concentration of OH•.

The degradation kinetics of pCBA by OH• can be described as

$$-\frac{d[pCBA]}{dt} = k_{\text{OH}\cdot\text{-pCBA}}[pCBA][\text{OH}\cdot] \quad (14)$$

where $k_{\text{OH}\cdot\text{-pCBA}}$ is the second-order rate constant of OH• with pCBA, [pCBA] is the concentration of pCBA, and [OH•] is the concentration of OH•.

The ratio of integration of Eq. 13 and Eq. 14 yields to equation below:

$$\frac{\ln\left(\frac{[IMI]_t}{[IMI]_0}\right)}{\ln\left(\frac{[pCBA]_t}{[pCBA]_0}\right)} = \frac{k_{\text{OH}\cdot\text{-IMI}}}{k_{\text{OH}\cdot\text{-pCBA}}} \quad (15)$$

The left-hand side of Eq. 15 is equal to the slope of the line shown in Fig. 6. The constant $k_{\text{OH}\cdot\text{-pCBA}}$ is given as 5 ×

Fig. 5 Reaction kinetics of IMI in different water matrices. ([IMI]₀ = 1000 μg L⁻¹ for Milli-Q water and VRMBR WW, [IMI]₀ = 332 μg L⁻¹ for Bio WW, UV lamp = 10 W (where applicable), O₃ dose = 1200 mg h⁻¹, O₃ flowrate = 30 L h⁻¹, pH = 7.25 ± 0.1, T = 24 °C ± 1 °C)

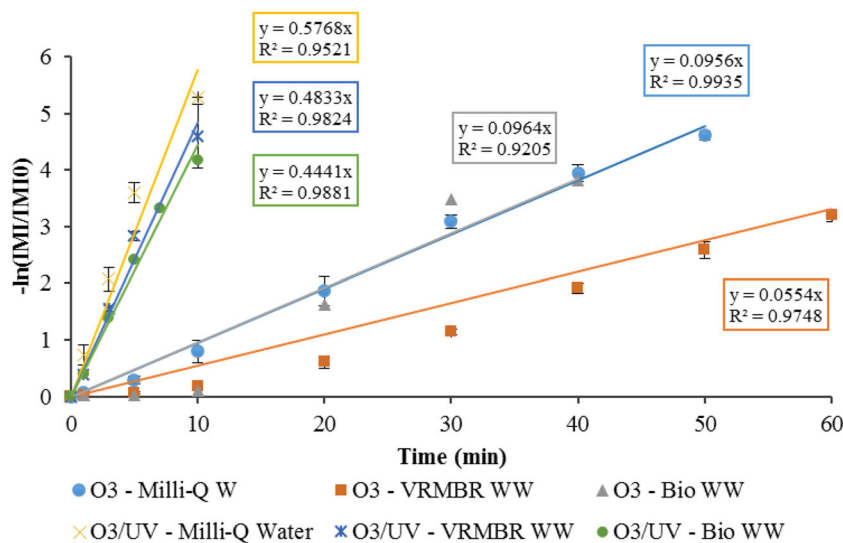
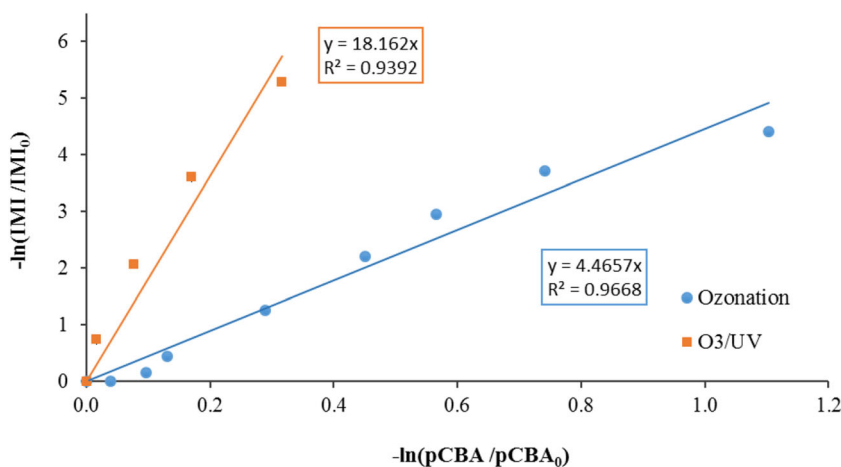


Fig. 6 IMI vs pCBA (Milli-Q water, $[pCBA]_0 = 5 \mu M$, $[IMI]_0 = 1000 \mu g L^{-1}$, O_3 dose = $1200 mg h^{-1}$, O_3 flowrate = $30 L h^{-1}$, $pH = 7.25 \pm 0.1$, $T = 24 \text{ }^\circ C \pm 1 \text{ }^\circ C$)



$10^9 M^{-1} s^{-1}$ (Elovitz and von Gunten 1999). For O_3/UV oxidation, the ratio of $k_{OH\cdot-IMI}/k_{OH\cdot-pCBA}$ is $18.162 M^{-1} s^{-1}$, and hence, the second-order rate constant for IMI oxidation by $OH\cdot$ ($k_{OH\cdot-IMI}$) is calculated as $9.08 \times 10^{11} M^{-1} s^{-1}$. For ozonation alone, the ratio of $k_{OH\cdot-IMI}/k_{OH\cdot-pCBA}$ is $4.4657 M^{-1} s^{-1}$ and hence $k_{OH\cdot-IMI}$ is $2.23 \times 10^{11} M^{-1} s^{-1}$. So, $k_{OH\cdot-IMI}$ in O_3/UV is much higher than O_3 . This could be another evidence for that IMI is highly reactive toward $OH\cdot$ since the production of $OH\cdot$ was boosted during the O_3/UV process.

Chen et al. (2018) found the second-order rate constant for $OH\cdot$ as $2.92 \times 10^9 M^{-1} s^{-1}$ during the ozonation of IMI at pH 6.97. The difference between the reaction rates found during our study and the referenced study could be due to different experimental conditions. Chen et al. (2018) investigated batch ozonation of IMI and applied different pH values than our study. Since the ozone was continuously supplied in this study, the $OH\cdot$ could be much higher than the referenced study. Furthermore, the effect of pH was pronounced, and it highly affected the production of $OH\cdot$. Since the pH in this study (7.25 ± 0.1) was higher than the one in the referenced study (6.97), the production of $OH\cdot$ could be higher in our study.

Mechanism of IMI degradation

IMI could be oxidized by directly and/or indirectly during ozonation. While the former one represents degradation by the ozone alone process, the latter is for the degradation by both ozone and radicals (Hoigne and Bader 1976). To find out the IMI degradation mechanism, whether it is dominated by direct or indirect mechanisms, Tert-butanol (TBA), which is a well-known $OH\cdot$ scavenger, was added (100 mM) during ozonation of IMI, as also suggested by Chen et al. (2016). TBA is used since the rate of TBA oxidation with ozone is very slow ($k_{O_3-TBA} = 1 \times 10^3 M^{-1} s^{-1}$), but it quickly reacts with $OH\cdot$. This shows that IMI is an ozone-resistant compound. For the investigation of $OH\cdot$ contribution on the IMI

disappearance during ozonation, experiments were presented with and without TBA. The ozone dose of $1200 mg h^{-1}$ was applied to Milli-Q water with a spike of IMI at $pH 7.25 \pm 0.1$, and the results presented in Fig. 7 were obtained.

As depicted from Fig. 7, at all sampling times, the IMI removal by the $O_3/OH\cdot$ mechanism was better than that by the O_3 mechanism for both O_3 and O_3/UV processes. Indeed, the difference was observed at the very beginning of the ozonation, even at the 1st min. This could be explained by the fact that $OH\cdot$ was simultaneously formed as the ozone is dissolved in the aqueous solution, and IMI readily reacted with $OH\cdot$. These results indicated that $OH\cdot$ is the dominant oxidizing

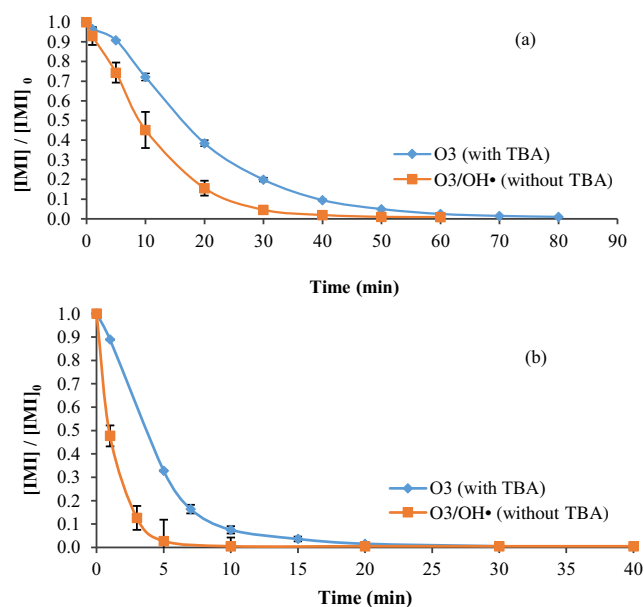


Fig. 7 Time course variation of IMI concentration by O_3 and $O_3/OH\cdot$, i.e., with and without TBA addition, respectively, for **a** ozonation (Milli-Q water, $[TBA] = 100 mM$ (where appropriate), $[IMI]_0 = 1000 \mu g L^{-1}$, O_3 dose = $1200 mg h^{-1}$, O_3 flowrate = $30 L h^{-1}$, $pH = 7.25 \pm 0.1$, $T = 24 \pm 1 \text{ }^\circ C$) and **b** photo-ozonation (Milli-Q water, $C_{TBA} = 200 mM$ (where appropriate), $[IMI]_0 = 1000 \mu g L^{-1}$, UV lamp = 10 W, O_3 dose = $1200 mg h^{-1}$, O_3 flowrate = $30 L h^{-1}$, $pH = 7.25 \pm 0.1$, $T = 24 \pm 1 \text{ }^\circ C$)

species to degrade IMI, and the oxidation via indirect mechanism by $\text{OH}\cdot$ was highly effective during ozonation.

Another reason for low degradation efficiency with TBA addition (i.e., O_3 -only mechanism) could be due to the chemical structure of IMI. As given previously (Fig. 1), IMI has two primary moieties, including a chloro-pyridine ring and an imidazolidine ring. The chloro-pyridine ring contains nitrogen and chlorine atoms with high electronegativity, which is not easily oxidized by electrophilic ozone. The finding that IMI oxidation is mostly by indirect oxidation is in agreement with the previous studies. Chen et al. (2018) showed that the degradation of IMI by ozonation highly depends on the concentration of $\text{OH}\cdot$. Another study by Cruz-Alcalde et al. (2017) indicated that a pesticide, namely Acetamiprid (ACMP), which belongs in the same chemical class (neonicotinoid) with IMI, is oxidized by $\text{OH}\cdot$ instead of ozone during ozonation. They introduced 25 mM of TBA into the reactor to investigate the degradation mechanism of ACMP and showed that TBA addition almost blocked the degradation of ACMP since its reaction rate with ozone was extremely low. Indeed, the common feature of IMI and ACMP is to contain chloro-pyridine ring in their chemical structure. So, these findings confirm that when a pollutant contains high electronegative moiety, it is mainly degraded by $\text{OH}\cdot$ instead of ozone during ozonation.

Ozonation by-products of IMI

Ozonation may result in incomplete degradation of pesticide molecules, and this may cause undesirable degradation by-products formation (Ikehata and El-Din 2005). Therefore, the possible IMI degradation pathway and the potential ozonation by-products of IMI was investigated.

First of all, during the initial stages of the ozonation study, two by-products (BP-1 and BP-2) were detected by HPLC. These two by-products were named as By-product-1 (BP-1) and By-product-2 (BP-2) since the exact chemical structures were not known. Profiles of BP-1 and BP-2 with respect to different ozone doses (600, 1200, and 1800 mg h^{-1}) are presented in Fig. 8a and b, respectively. Although IMI was immediately degraded from the first minute of ozonation, these two by-products did not appear simultaneously.

As seen from Fig. 8a, in all ozone doses, BP-1 was observed starting from the 5th min. It reached its maximum area around 110 min for both 1200 and 1800 mg h^{-1} ozone doses, whereas the plateau was not reached within 180 min for 600 mg h^{-1} ozone dose. To add more, during the ozonation of BP-1, the areas obtained in the 1200 and 1800 mg h^{-1} ozone dose experiments were similar. This indicates that the increase in ozone dose did not significantly affect the amount formation of BP-1. On the contrary, the area of BP-1 at 600 mg h^{-1} ozone dose application was relatively smaller than those of the other ozone doses. While IMI was degraded

below its LoD value (99% disappearance) within 110, 60, and 50 min, for 600, 1200, and 1800 mg h^{-1} ozone doses, respectively, BP-1 continued to present after 180-min ozonation for the same ozone doses.

Similar to BP-1, BP-2 was also presented, starting from the 5th min (Fig. 8b). BP-2 reached to its maximum area sooner but having a lower area than the BP-1. As the ozone doses were increased, BP-2 reached to its maximum area faster and started to lessen as proportional to ozone doses. BP-2 was almost not detected after 150 min of ozonation for 1200 and 1800 mg h^{-1} ozone doses. On the other hand, 180 min was not enough to remove almost all of BP-2 for the 600 mg h^{-1} ozone dose.

It can be inferred from Fig. 8a and b that while 110, 60, and 50 min required to degrade 99% of IMI for 600, 1200, and 1800 mg h^{-1} ozone doses, respectively, more than 180 min was required for the disappearance of BP-1 and BP-2. Moreover, the greatest concern regarding the incomplete degradation of by-products is due to the effect of these by-products on the aquatic environment. Unfortunately, oxidation by-products might be more toxic than the parent compound (Rizzo 2011). Therefore, the toxicity of the treated solution should also be taken into consideration, and it should be further investigated. It should be pointed here that there may be other by-products that are not detectable by HPLC. Accordingly, a study concerning these other possible by-products was conducted using LC-MS/MS at a constant ozone dose.

For the by-products that could not be detected by HPLC, the LC-MS/MS chromatograms of IMI ozonation in Milli-Q water and VRMBR WW were obtained (Supplementary Fig. 1–5). For all the samples, m/z 99 and 195 ions were detected due to the presence of phosphate buffer in the Milli-Q water. Another ion, m/z 239, was detected in all the samples with an almost constant concentration, which may show that this ion could have occurred due to impurities in the samples. For this reason, these ions were neglected during the evaluation of the IMI degradation pathway and produced by-products.

An IMI degradation pathway was proposed based on the fragmentation of m/z 256 in the LC-MS/MS (Supplementary Fig. 1). As depicted from Fig. 9, IMI lost N_2O and formed m/z 212 fragment ion. Similarly, due to the loss of HNO_2 from IMI, the fragment ion m/z 209 formed. The other way represents that IMI consecutively lost NO_2 and Cl and the fragment ions m/z 210 and m/z 175 formed, respectively. Although m/z 210 did not clearly occur in our fragmentation study, Bourgin et al. (2011) showed this ion is a precursor of m/z 175. Therefore, the m/z 210 ion is shown with the red dashed line in Fig. 9.

In following the IMI degradation by O_3 using LC-MS/MS, the chromatograms belonging to 5-, 70-, and 180-min reaction times were analyzed. Supplementary Fig. 2 and 3 present the

Fig. 8 Time course variation of **a** IMI and BP-1 and **b** IMI and BP-2 at different ozone doses (Milli-Q water, $[IMI]_0 = 500 \mu\text{g L}^{-1}$, O_3 flowrate = 30 L h^{-1} , $\text{pH} = 7.25 \pm 0.1$, $T = 24 \text{ }^\circ\text{C} \pm 1 \text{ }^\circ\text{C}$)

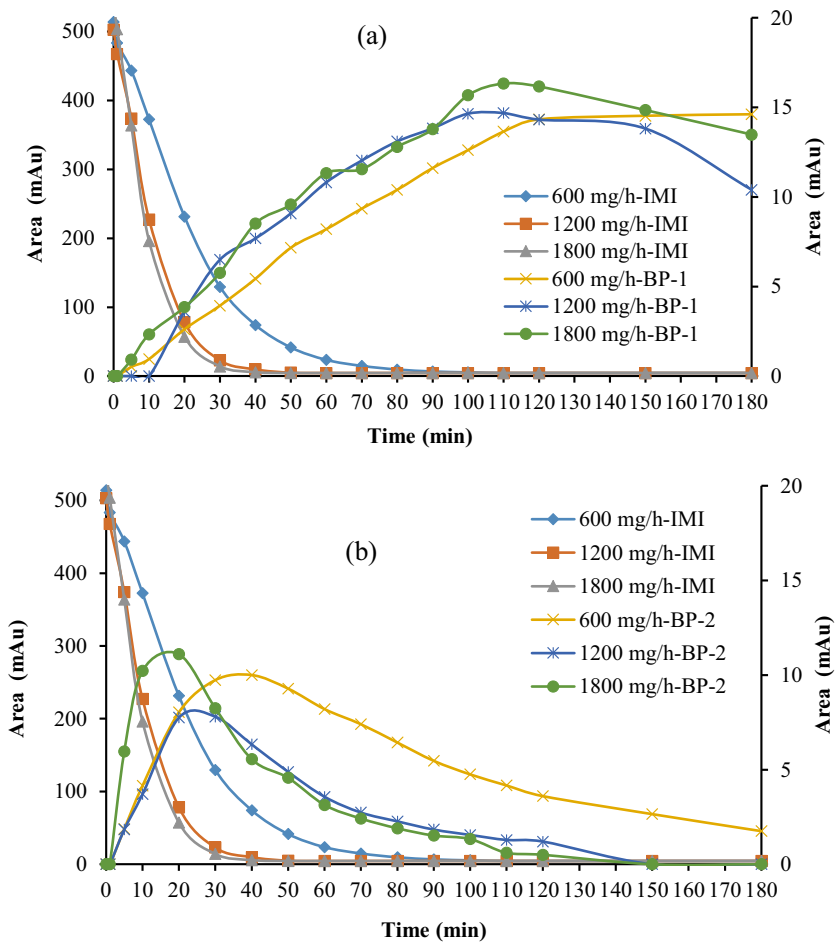
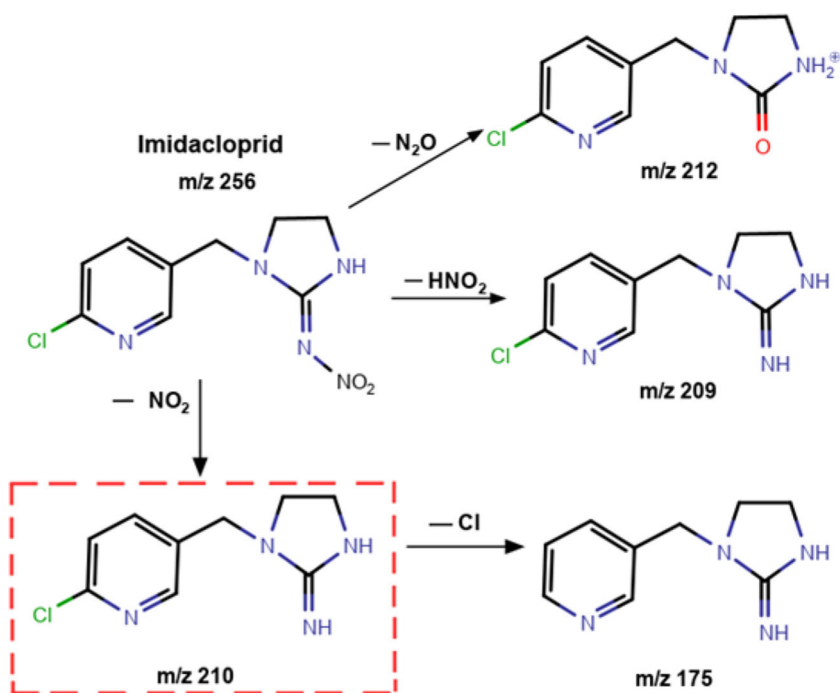


Fig. 9 The proposed fragmentation pathway for IMI (dashed line represents the precursor ion for m/z 175 formation as stated by Bourgin et al. 2011)



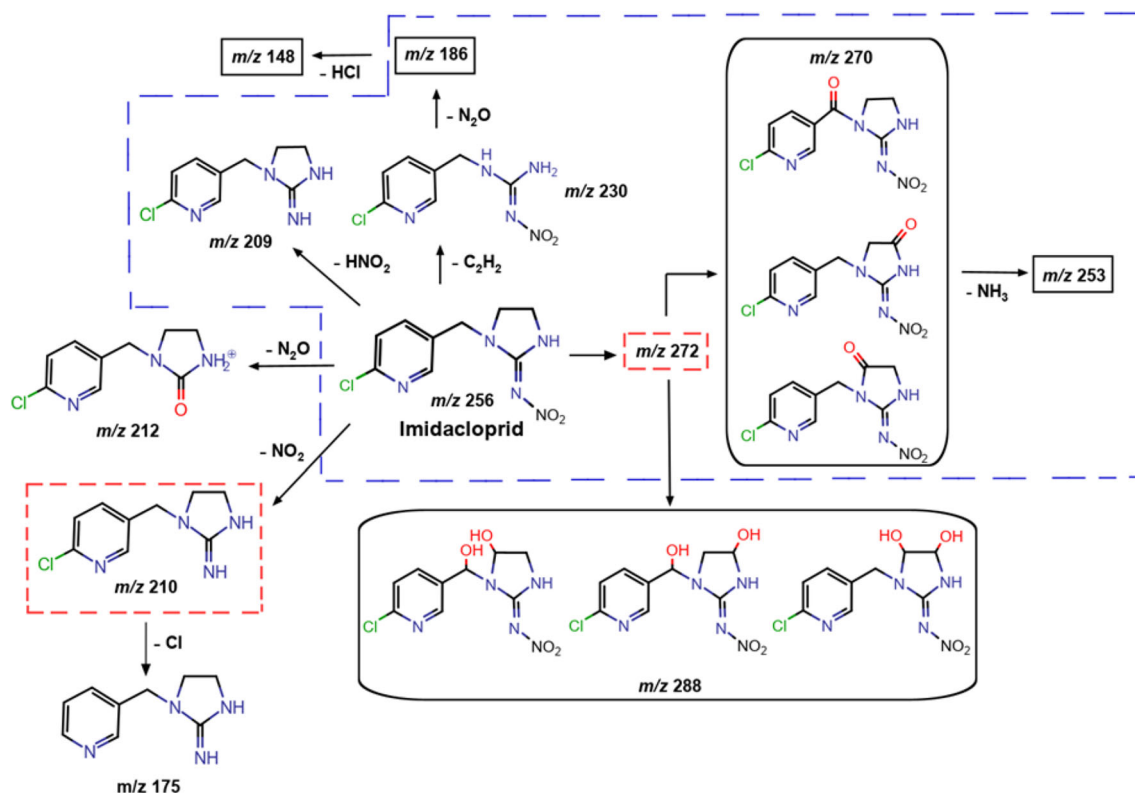


Fig. 10 The proposed degradation pathway of IMI by O_3 and O_3/UV (by-products within the blue dashed line are common for both O_3 and O_3/UV processes whereas those within the red dashed line are adopted from Bourgin et al. 2011)

chromatograms for Milli-Q water and VRMBR WW, respectively. Based on these observations, the IMI degradation pathway was proposed, as shown in Fig. 10. IMI (m/z 256) significantly decreased after 70 min ozonation. After 180 min of ozonation, IMI slightly occurred, which could correspond to below LoD value in the HPLC. As IMI (m/z 256) degraded, m/z 209 and m/z 253, increased in 70-min ozonation, but then they decreased to some degree. Indeed, 180 min of ozonation was not enough to remove these by-products. Moreover, m/z 270 was generated within the first 5 min of treatment; it gradually decreased and eventually disappeared after 180 min of ozonation (Supplementary Fig. 2).

Similar to Bourgin et al. (2011), the opening of the imidazoline ring produced a by-product, which was detected at m/z 230 during the ozonation of Milli-Q water. Indeed, IMI lost C_2H_2 during the formation of m/z 230. Fragmentation of m/z 230 yielded to m/z 186 and m/z 148. The fragment ion at m/z 186 was obtained by loss of N_2O , whereas the fragment ion at m/z 148 was observed by the consecutive loss of N_2O and HCl similar to the referenced literature.

IMI (m/z 256) ozonation yielded to m/z 270. Carbonylated forms of IMI could have resulted in the detection of m/z 270 ions, which were also mentioned by Bourgin et al. (2011). The three possible chemical structures for m/z 270 are given in Fig. 10. On the other hand, different from the referenced study, fragmentation of m/z 270 yielded m/z 253 ion by the

loss of NH_3 in our study. Moreover, the dehydroxylated form of IMI, which was also proposed by the referenced study, gives the fragment ion at m/z 288. The three possible chemical structures for m/z 288 are given in Fig. 10. Bourgin et al. (2011) stated that before the carbonylated and dehydroxylated forms of IMI were produced, monohydroxylation of IMI was detected with an ion at m/z 272. It is worth noting that, unlike Bourgin et al. (2011), m/z 272 ion was not detected in our study. The reason could be a quick transformation of m/z 272 into m/z 270 and m/z 288 ions. The anticipated m/z 272 ion is indicated by the red dashed line in Fig. 10.

As can be seen from the m/z values mentioned above, during ozonation, in total 11 by-products with fragmented ions were detected by LC-MS/MS. However, after treatment, only m/z 270 ion was disappeared entirely. Unfortunately, it was not possible to match BP-1 and BP-2 (detectable by HPLC) with those detected by LC-MS/MS due to differences in both types of equipment and methods used. Nevertheless, it is for sure that any two of 11 by-products were corresponding to BP-1 and BP-2.

Unlike for the ozonation case, no by-products were detected by HPLC at the end of the photo-ozonation experiment. On the other hand, there were still present by-products detected by LC-MS/MS, though smaller in number than in ozonation case. However, some by-products, namely m/z 186, m/z 209, m/z 230, m/z 253, and m/z 270, were common in both cases. A

comparative presentation of the degradation pathways for O₃ and O₃/UV process is provided in Fig. 10. Observing a smaller number of by-products in photo-ozonation can be considered as another indication of better performance of photo-ozonation as compared to ozonation.

In both Milli-Q water and VRMBR WW, IMI (m/z 256) was not detected (Supplementary Fig. 4 and 5, respectively), which shows that O₃/UV is a successful treatment application for IMI removal. Moreover, the m/z 209 ion, which was also detected during IMI fragmentation in the ozonation case, was also detected during O₃/UV, but it disappeared after 60 min of treatment. It could be either generated by subtracting HNO₂ from IMI (Bourgin et al. 2011) or protonated form of IMI olefin desnitro (Ding et al. 2011). Although Ding et al. (2011) studied by-products of IMI photolysis, they observed protonated form of IMI olefin desnitro. In addition to m/z 209 ions, m/z 206 ion was also detected at the almost same level with m/z 209 ions. However, since the m/z 206 ion was detected in the phosphate buffer solution, this ion was not taken into account while evaluating the IMI degradation pathway and produced by-products.

The m/z 253 ion, which was also detected during IMI fragmentation in the ozonation case, was detected during O₃/UV in both Milli-Q water and VRMBR WW. After 60 min of treatment, the m/z 253 ion decreased to some degree, but it was not completely removed (Supplementary Fig. 4 and 5, respectively). This suggests that m/z 253 ion may be the last step degradation by-product.

The ion at m/z 186 was observed in only the Milli-Q water case. During O₃/UV, m/z 186 ion appeared from the very beginning (5 min of treatment), then decreased and eventually disappeared. The presence of m/z 186 could be via fragmentation of m/z 230, which was mentioned as the way of m/z 186 production during ozonation (Supplementary Fig. 4). However, m/z 230 was not detected during O₃/UV. Indeed, this could show that it might be quickly transformed into m/z 186 within the first 5 min of treatment. Moreover, the ion at m/z 270, which was also detected during ozonation, decreased continuously during O₃/UV in the VRMBR WW and disappeared to signal noise level ($< 1 \times 10^4$ area) after 60 min of treatment (Supplementary Fig. 5). Hence, these studies showed that only 4 by-products were observed, and just one of them (m/z 253) remained during O₃/UV.

Although Moza et al. (1998), Wamhoff and Schneider (1999), and Ding et al. (2011) reported 6-chloronicotinic acid as a major degradation product of IMI, we did not detect 6-chloronicotinic acid in our study. One of the reasons could be the low [IMI]₀ tested. Another reason that was stated by Ding et al. (2011), 6-chloronicotinic acid is far more sensitive to negative ion ESI mode, whereas our results were obtained in the positive ion ESI mode.

Conclusion

The following conclusions could be drawn from this study:

- The ozonation, coupled with UV accelerated IMI removal by ozone alone, remarkably, regardless of the wastewater matrix. Almost complete IMI disappearance is achieved within only 10 min.
- The indirect mechanism (by OH•) dominated the IMI disappearance by ozonation. The rate constants of IMI degradation by O₃/OH• and O₃-only were calculated as 0.0956 and 0.0595 min⁻¹, respectively.
- The kinetic study proved that the IMI degradation rate by O₃/UV was 4.6–8.7 times higher than by O₃ alone, depending on operational conditions and water matrix.
- The water matrix effect on IMI removal was more pronounced during the O₃ process than O₃/UV.
- Fewer by-products were formed in the case of O₃/UV than O₃ alone.

Acknowledgments The authors thank Middle East Technical University (METU) Central Laboratory for the LC-MS/MS analysis. We also thank Dr. Tamay Seker for her contribution to the evaluation of LC-MS/MS chromatograms.

Funding information This study was financially supported by The Scientific and Technological Research Council of Turkey (TUBITAK) via the project number 115Y013.

References

- Acero JL, Von Gunten U (2001) Characterization of oxidation processes: ozonation and the AOP O₃/H₂O₂. *J AWWA* 93:90–100
- Antoniou MG, Hey G, Vega SR, Spiliotopoulou A, Fick J, Tysklind M, Jansen JC, Andersan HR (2013) Required ozone doses for removing pharmaceuticals from wastewater effluent. *Sci Total Environ* 456: 42–49
- Benitez F, Acero J, Real F, Roldan G (2009) Ozonation of pharmaceutical compounds: rate constants and elimination in various water matrices. *Chemosphere* 77:53–59
- Bolton JR, Stefan MI, Shaw PS, Lykke KR (2011) Determination of the quantum yields of the potassium ferrioxalate and potassium iodide-iodate actinometers and a method for the calibration of radiometer detectors. *J Photochem Photobiol A Chem* 222:166–169
- Bourgin M, Violleau F, Debrauwer L, Albet J (2011) Ozonation of imidacloprid in aqueous solutions: reaction monitoring and identification of degradation products. *J Hazard Mater* 190:60–68
- Cernigoj U, Stangar UL, Trebse P (2007) Degradation of neonicotinoid insecticides by different advanced oxidation processes and studying the effect of ozone on TiO₂ photocatalysis. *Appl Catal B* 75:229–238
- Cerreta G, Roccamante MA, Oller I, Malato S, Rizzo L (2019) Contaminants of emerging concern removal from real wastewater by UV/free chlorine process: a comparison with solar/free chlorine and UV/H₂O₂ at pilot scale. *Chemosphere* 236, Article 124354

- Chávez AM, Ribeiro AR, Moreira NFF, Silva AMT, Rey A, Álvarez PM, Beltrán FJ (2019) Removal of Organic Micropollutants from a Municipal Wastewater Secondary Effluent by UVA-LED Photocatalytic Ozonation. *Catalysts* 9 (5):472
- Chelme-Ayala P, El-Din MG, Smith DW (2010) Kinetics and mechanism of the degradation of two pesticides in aqueous solutions by ozonation. *Chemosphere* 78:557–562
- Chen Z, Fang J, Fan C, Shang C (2016) Oxidative degradation of N-nitrosopyrrolidine by the ozone/UV process: kinetics and pathways. *Chemosphere* 150:731–739
- Chen S, Deng J, Deng Y, Gao N (2018) Influencing factors and kinetic studies of imidacloprid degradation by ozonation. *Environ Technol* 40:2127–2134
- Cruz-Alcalde A, Sans C, Esplugas S (2017) Priority pesticides abatement by advanced water technologies: the case of acetamiprid removal by ozonation. *Sci Total Environ* 599–600:1454–1461
- Dani VD, Lankadurai BP, Nagato EG, Simpson AJ, Simpson MJ (2019) Comparison of metabolomic responses of earthworms to sub-lethal imidacloprid exposure in contact and soil tests. *Environ Sci Pollut Res* 26:18846–18855
- Ding T, Jacobs D, Lavine BK (2011) Liquid chromatography-mass spectrometry identification of imidacloprid photolysis products. *Microchem J* 99:535–541
- Elovitz M, von Gunten U (1999) Hydroxyl radical/ozone ratios during ozonation processes. I. The Rct concept. *Ozone-Sci Eng* 21:239–260
- Fernandes E, Martins RC, Gomes J (2020) Photocatalytic ozonation of parabens mixture using 10% N-TiO₂ and the effect of water matrix. *Sci Total Environ* 71820:Article 137321. <https://doi.org/10.1016/j.scitotenv.2020.137321>
- Fijolek L, Nawrocki J (2018) Phosphate helps to recover from scavenging effect of chloride in self-enhanced ozonation. *Chemosphere* 212:802–810
- Gardoni D, Vailati A, Canziani R (2012) Decay of ozone in water: a review. *Ozone-Sci Eng* 34:233–242
- Genç N, Doğan E, Narci E, Bican E (2017) Multi-response optimization of process parameters for imidacloprid removal by reverse osmosis using Taguchi design. *Water Environ Res* 89:440–450
- Gomes J, Costa R, Quinta-Ferreira RM, Martins RC (2017) Application of ozonation for pharmaceuticals and personal care products removal from water. *Sci Total Environ* 58615:265–283
- Henze M (1992) Characterization of wastewater for modelling of activated sludge processes. *Water Sci Technol* 25(6):1–15
- Hoigne J, Bader H (1976) The role of hydroxyl radical reactions in ozonation processes in aqueous solutions. *Water Res* 10:377–386
- Hoigne J, Bader H (1983) Rate constants of reactions of ozone with organic and inorganic compounds in water. *Water Res* 17:173–183
- Ikehata K, El-Din MG (2005) Aqueous pesticide degradation by ozonation and ozone-based advanced oxidation processes: a review (part I). *Ozone-Sci Eng* 27:83–114
- Jeschke P, Nauen R, Schindler M, Elbert A (2010) Overview of the status and global strategy for neonicotinoids. *J Agric Food Chem* 59:2897–2908
- Kanwal M, Tariq SR, Chotana GA (2018) Photocatalytic degradation of imidacloprid by Ag-ZnO composite. *Environ Sci Pollut Res* 25:27307–27320
- Kocaman K (2019) Fate and removal of pesticides in wastewater treatment plants-case of Yeşilirmak Basin, MSc Thesis, Ankara METU <http://etd.lib.metu.edu.tr/upload/12623100/index.pdf>
- Liu Z, Yang Y, Shao C, Ji Z, Van Hulle S (2020) Ozonation of trace organic compounds in different municipal and industrial wastewaters: kinetic-based prediction of removal efficiency and ozone dose requirements. *Chem Eng J Article* 387 123405. <https://doi.org/10.1016/j.cej.2019.123405>
- Loos R, Dimitar Marinov, Isabella Sanseverino, Dorota Napierska and Teresa, Lettieri, (2018) Review of the 1st Watch List under the Water Framework Directive and recommendations for the 2nd Watch List, EUR 29173 EN, Publications Office of the European Union, Luxembourg, ISBN 978–92–79–81839–4, doi:<https://doi.org/10.2760/614367>, JRC111198
- Lucas M, Peres J, Puma G (2010) Treatment of winery wastewater by ozone-based advanced oxidation processes (O₃, O₃/UV, and O₃/UV/H₂O₂) in a pilot-scale bubble column reactor and process economics. *Sep Purif Technol* 72:235–241
- Malato S, Blanco J, Cacered J, Fernandez-Alba A, Agüera A, Rodriguez A (2002) Photocatalytic treatment of water-soluble pesticides by photo-Fenton and TiO₂ using solar energy. *Catal Today* 76:209–220
- Mandal A, Singh N (2017) Optimization of atrazine and imidacloprid removal from water using biochars: designing single or multi-staged adsorption systems. *Int J Hyg Environ Health* 220:637–645
- Moza P, Hustert K, Feicht E, Kettrup A (1998) Photolysis of imidacloprid in aqueous solution. *Chemosphere* 36:497–502
- Nakada N, Shinohara H, Murata A, Kiri K, Managaki S, Sato N, Takada H (2007) Removal of selected pharmaceuticals and personal care products (PPCPs) and endocrine-disrupting chemicals (EDCs) during sand filtration and ozonation at a municipal sewage treatment plant. *Water Res* 41:4373–4382
- Oktem YA, Yuzer B, Aydin MI, Okten HE, Selcuk H (2019) Chloride or sulfate? Consequences for ozonation of textile wastewater. *J Environ Manag* 2471:749–755
- Oller I, Malato S, Sánchez-Pérez JA (2011) Combination of advanced oxidation processes and biological treatments for wastewater decontamination -a review. *Sci Total Environ* 409 (2015):4141–4166
- Phattarapattamawong S, Kaiser AM, Saracevic E, Schaar HP, Krampe J (2017) Optimization of ozonation and peroxone process for simultaneous control of micropollutants and bromate in wastewater. *Water Sci Technol* 2:404–411. <https://doi.org/10.2166/wst.2018.170>
- Prieto-Rodríguez L, Oller I, Klammerth N, Agüera A, Malato A (2013) Application of solar AOPs and ozonation for elimination of micropollutants in municipal wastewater treatment plant effluents. *Water Res* 47(415):1521–1528
- Rackness K, Gordon G, Langlais B, Masschelein W, Matsumoto N, Richard Y, Robson CM, Somiya I (1996) Guideline for measurement of ozone concentration in the process gas from an ozone generator. *Ozone-Sci Eng* 18:209–229
- Rajah Z, Guiza M, Solís RR, Becheikh N, Ouederni A (2019) Clopyralid degradation using solar-photocatalytic/ozone process with olive stone activated carbon. *J Environ Chem Eng* 7:1029004
- Raut-Jadhav S, Saharan V, Pinjari D, Saini D, Sonawane S, Pandit A (2013) Intensification of degradation of imidacloprid in aqueous solutions by combination of hydrodynamic cavitation with various advanced oxidation processes (AOPs). *J Environ Chem Eng* 1:850–857
- Reynolds G, Graham N, Perry R, Rice R (1989) Aqueous ozonation of pesticides-a review. *Ozone Sci Eng* 11:339–382
- Ribeiro AR, Nunes OC, Pereira MF, Silva AM (2015) An overview on the advanced oxidation processes applied for the treatment of water pollutants defined in the recently launched directive 2013/39/EU. *Environ Int J* 75:33–51
- Rizzo L (2011) Bioassays as a tool for evaluating advanced oxidation processes in water and wastewater treatment. *Water Res* 45:4311–4340
- Rizzo L, Krätke R, Linders J, Scott M, Vighi M, de Voogt P (2018) Proposed EU minimum quality requirements for water reuse in agricultural irrigation and aquifer recharge: SCHEER scientific advice. *Curr Opin Environ Sci Heal* 2:7–11
- Rózsa G, Náfrádi M, Alapi T, Schrantz K, Tungler A (2019) Photocatalytic, photolytic and radiolytic elimination of imidacloprid

- from aqueous solution: reaction mechanism, efficiency and economic considerations. *Appl Catal B Environ* 2505:429–439
- Schmitt A, Mendret J, Roustan M, Brosillon S (2020) Ozonation using hollow fiber contactor technology and its perspectives for micropollutants removal in water: a review. *Sci Total Environ* 72910:138664
- Segura C, Zaror C, Mansilla H, Mondaca M (2008) Imidacloprid oxidation by photo-Fenton reaction. *J Hazard Mater* 150:679–686
- Staehelin J, Hoigne J (1982) Decomposition of ozone in water: rate of initiation by hydroxide ions and hydrogen peroxide. *Environ Sci Technol* 16:676–681
- Tomlin CDS (2006) *The pesticide manual, a world compendium*, 14th Ed., Alton: British Crop Protection Council, pp. 598-599, England
- Vatankhah H, Riley SM, Murray C, Quiñones O, Steirer KX, Dickenson ERV, Bellona C (2019) Simultaneous ozone and granular activated carbon for advanced treatment of micropollutants in municipal wastewater effluent. *Chemosphere* 234:845–854
- Wamhoff H, Schneider V (1999) Photodegradation of imidacloprid. *J Agric Food Chem* 47:1730–1734
- Yao W, Rehman SWU, Wang H, Yang H, Yu G, Wang Y (2018) Pilot-scale evaluation of micropollutant abatements by conventional ozonation, UV/O₃, and an electro-peroxone process. *Water Res* 138:106–117
- Zhang Y, He P, Zhou L, Dong F, Zhou S (2020) Optimized terbium doped Ti/PbO₂ dimensional stable anode as a strong tool for electrocatalytic degradation of imidacloprid waste water. *Ecotoxicol Environ Saf* 18830:Article 109921. <https://doi.org/10.1016/j.ecoenv.2019.109921>
- Zhao HY, Qian L, Chen Y, Wang QN, Zhao GH (2018) Selective catalytic two-electron O₂ reduction for onsite efficient oxidation reaction in heterogeneous electro-Fenton process. *Chem Eng J* 332:486–484

Publisher's note Springer Nature remains neutral with regard to jurisdictional claims in published maps and institutional affiliations.